WNT2–SOX4 positive feedback loop promotes chemoresistance and tumorigenesis by inducing stem-cell like properties in gastric cancer

Xiang-Yu Tan[1], Yu-Ting Li[1,2], Hua-Hui Li[1,2], Li-Xiang Ma[1], Chui-Mian Zeng[3], Tian-Tian Zhang[1], Tu-Xiong Huang[1], Li Fu[1]

[1]Guangdong Province Key Laboratory of Regional Immunity and Diseases, Department of Pharmacology and Shenzhen University International Cancer Center, Shenzhen University Health Science Center, Shenzhen, China

[2]Shenzhen University-Friedrich Schiller Universitat Jena Joint PhD Program in Biomedical Sciences, Shenzhen University School of Medicine, Shenzhen, China

[3]Department of Endocrinology and Diabetes Center, The First Affiliated Hospital of Sun Yat-sen University, Guangzhou, Guangdong, China

Xiangyu Tan and Yuting Li contributed equally.

Corresponding Author: Li Fu, Department of Pharmacology and International Cancer Center, Shenzhen University Health Science Center, Shenzhen 518060, China; Email: gracelfu@szu.edu.cn

Running title: WNT2–SOX4 axis enhances gastric cancer tumorigenesis

Conflict of interest

The authors declare no potential conflict of interest.

Keywords: WNT2, SOX4, chemoresistance, stemness, gastric cancer

Supporting Information

Supplemental Methods

Lentivirus vectors, cell transfection, and lentiviral transduction

WNT2 (NM_003391.3), FZD8 (NM_031866.3), CTNNB1 (NM_001098209.2), and SOX4 (NM_003107.3)-specific shRNA expression vectors and scrambled shRNA NTC were manufactured by Guangzhou IGE Biotechnology Ltd. WNT2 (NM_003391.3), FZD8 (NM_031866.3), and SOX4 (NM_003107.3) overexpression and control vectors were manufactured by Guangzhou GeneCopoeia Biotechnology Ltd. The shRNA sequences and overexpression CDS sequences used are listed in Supplementary materials. To generate lentiviral particles, pCMV-VSVG and psPAX2 envelope and packaging plasmids were co-transfected into 293T cells with the custom lentiviral plasmids using Lipofectamine 3000 Reagent (Invitrogen) following the manufacturer's protocol. Virus-containing supernatant was collected 48 h later, filtered with a 0.45-μm filter, and concentrated with a Lenti-X Concentrator (Takara). To establish stable transfection clones, the target cells were infected with lentiviral particles, subsequently selected by puromycin (Sigma, 10 ug/ml), and maintained in a medium containing the indicated concentration. Cells were harvested for qPCR and western blotting analysis to verify the expression of targeted genes 48-72 h after transfection.

Western blotting

Western blotting was performed according to the standard protocol. Cultured cells were lysed in radioimmunoprecipitation assay (RIPA) buffer (Beyotime) with protease and phosphatase inhibitors (Cell Signaling Technology). Total protein concentration was determined via BCA assay (Thermo Fischer Scientific). Cell lysates were separated on SDS-polyacrylamide gels (Epizyme) and then transferred onto polyvinylidene difluoride (PVDF; Bio-Rad) membranes. After the membranes were blocked in 10% BSA for 2 h, they were incubated with primary antibodies overnight at 4 °C and with secondary antibodies for 2 h at room temperature. The antibodies used

in the western blot are listed in the Supplementary Materials. Finally, the immunoblots were visualized by using Pierce SuperSignal west chemiluminescent substrate (Thermo Scientific) and the ChemiDoc Touch Gel Imaging system (Bio-Rad). Protein band intensity was quantified using Image Lab software (Bio-Rad).

RNA Extraction and qPCR

Total RNA was extracted using TRIzol Reagent (Invitrogen) and reversed-transcribed with PrimeScript RT-PCR Master Mix (Takara) using standard procedures. Real-time (q)PCR for analyzing mRNA levels was performed with TB Green Premix Ex Taq (Takara) on a CFX96 Real-Time PCR Detection System (Bio-Rad). The amplification protocol consisted of incubations at 95 °C for 15 s, 60 °C for 1 min, and 72 °C for 1 min for 40 cycles. Data then were normalized to the level of GAPDH mRNA in each sample. The forward and reverse oligonucleotide primers containing single-nucleotide alterations are listed in the Supplementary Materials. Fold change in expression was analyzed according to the $2^{-\Delta\Delta Ct}$ method.

Cell proliferation assay

The cell counting kit (CCK)-8 method was used to detect cell viability. Exponentially growing cells were seeded into 96-well plates at a density of 2×10^3 to 5×10^3 cells/well with a total of 100 μL medium. The absorbance at 450 nm wavelength was measured using a microplate reader (Biotek) after cultivating cells with 10 μL/well CCK-8 reagent (Dojindo Kumamoto) for 4 h. The same protocol was used for all time points. The half-maximal inhibitory concentrations (IC50 values) were calculated using GraphPad Prism software (GraphPad, Version 8.0).

Spheroid-formation assay

Single cells used for the tumor sphere formation assay were cultured in suspension in ultra-low attachment 6-well plates (Corning) at a density of 100 cells/well using GCSC complete culture medium for 1 week. Cells were replenished with fresh medium every 3 days. Images of the spheroids were visualized via the inverted microscope (Zeiss).

ELISA

The GCSC supernatant concentrations of WNT2 were measured using human WNT2 (CUSABIO, CSB-EL026133HU), according to the manufacturer's instructions.

Limiting dilution in vitro assay

GCSC diluted to defined doses (1 cell/100 mL to 80 cells/100 mL) were plated onto flat bottom ultra-low-attachment 6-well plates (Corning) in GCSC complete culture medium. The number of seeded cells and positive tumor spheroids were used to determine the “tumor-initiating cell frequency” and were analyzed with the extreme limiting dilution analysis “limdil” function (http://bioinf.wehi.edu.au/software/elda/index.html/) (1) after 2 weeks of culture.

Co-immunoprecipitation and ubiquitination assay

For the co-immunoprecipitation (co-IP) and ubiquitination assays, cells were lysed with RIPA buffers (Invitrogen) supplemented with protease and phosphatase inhibitors (Cell Signaling Technology). Approximately 1000-1500 mg of whole-cell lysates (co-IP) were incubated overnight at 4 °C with anti-DYKDDDDK Tag (Cell Signaling Technology) or anti-HA antibody (Cell Signaling Technology) for the co-IP assay and anti-ubiquitin (Proteintech) for the ubiquitination assay followed by precipitation of the antibody–protein complex using protein A/G-agarose beads (Invitrogen). A matched isotype antibody (IgG; Cell Signaling Technology) was used as a negative control. After washing four times with lysis buffer, the precipitated protein complexes were eluted with 1 × loading buffer and boiled for 5 min followed by western blot analysis.

Flow cytometry

GCSCs were incubated with FITC-conjugated anti-CD44 antibody (Biolegend) or APC-conjugated anti-CD54 antibody (Biolegend) followed by CytoFLEX system (Beckman Coulter) and Kaluza software analysis.

Gene set enrichment analysis, Kaplan–Meier analysis, and statistical analysis

The mRNA expression data and clinical information related to the stomach adenocarcinoma dataset were derived from TCGA. For GSEA, 415 gastric cancer samples from the TCGA database. Then, the whole-genome expression profile was loaded into GSEA software (http://software.broadinstitute.org/gsea/index.jsp) for analysis. Statistical significance data of qPCR, sphere formation assay, invasion and

migration assays, limiting dilution in vitro assay, ELISA, Cell proliferation assay, flow cytometry analysis were performed using an unpaired two-tailed Student's *t*-test for analysis for two groups or two-way ANOVA for analysis of multiple groups using GraphPad Prism software (GraphPad, Version 8.0). The Wilcoxon test or Kruskal-Wallis test were adjusted for non-parametric tests of non-normal distribution groups. Kaplan–Meier Plots and a log-rank test was used for analyzing overall survival. The χ^2 test was used to assess the correlations between WNT2 and SOX4 expression and clinicopathological parameters. The error bars are presented as the means ± SD. A *P*-value less than 0.05 was considered significant.

Data availability

The raw scRNA-seq data for gastric cancer samples used to extend our analyses were extracted from a dataset (accession number: GSE183904) in the National Center for Biotechnology Information's Gene Expression Omnibus database repository (GEO database: https://www.ncbi.nlm.nih.gov/geo/). R software is a free software environment for statistical computing and graphics (https://www.r-project.org). The corresponding author's data and the computer code used and analyzed in this study are available upon reasonable request.

Supplementary Figures & Legends

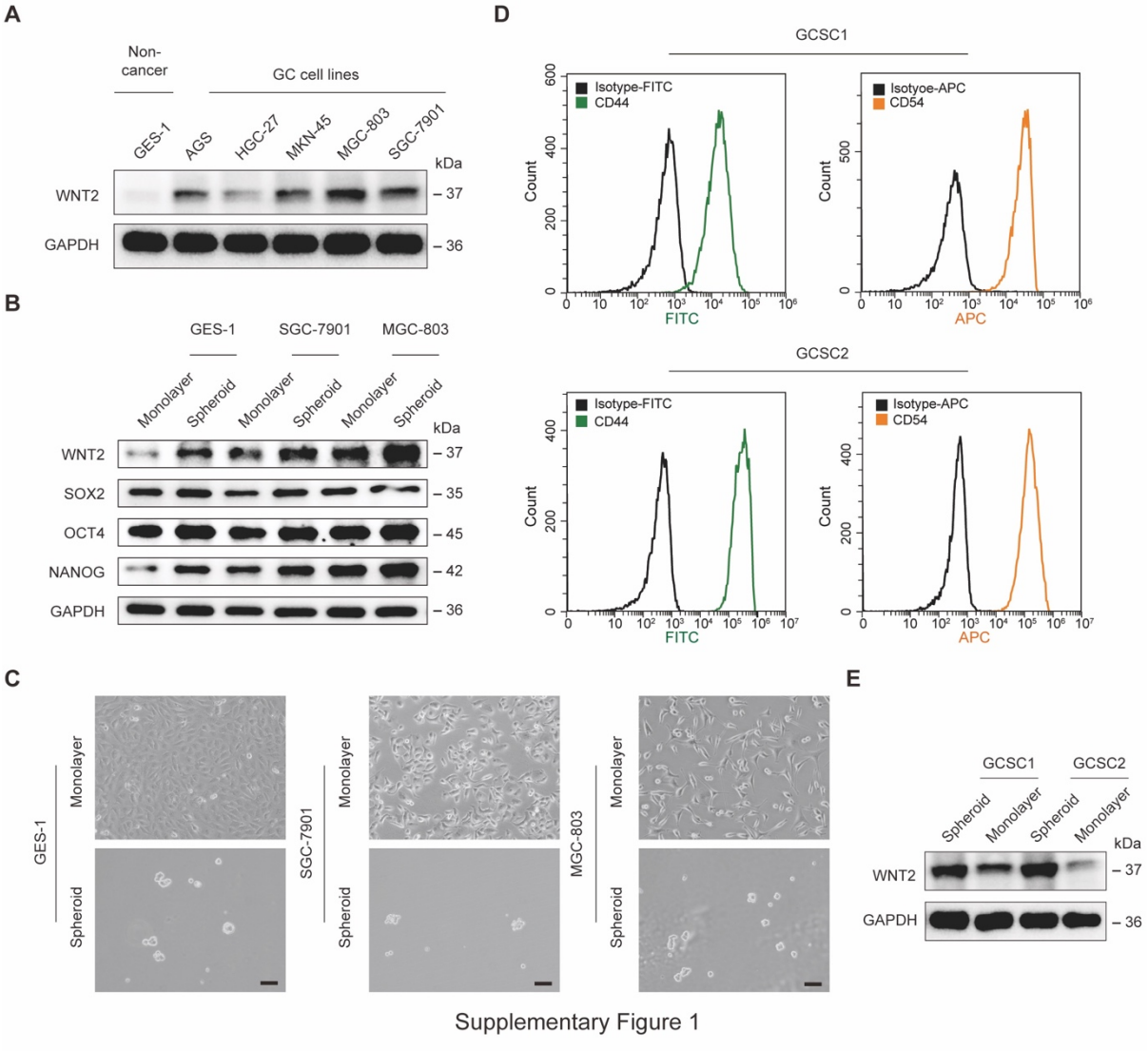

Supplementary Figure 1

Supplementary Fig. 1 Overexpression of WNT2 is associated with stemness properties in GC (Related to Fig. 1)

A, Western blot analysis of WNT2 protein expression in an immortalized normal gastric epithelial cell line (GES-1) and GC cell lines (AGS, HGC-27, MKN-45, MGC-803, SGC-7901). **B,** Western blot examination of WNT2 and stemness-related protein levels in GES-1, SGC-7901, and MGC-803 grown as monolayer versus spheroids. **C,** Representative images of the morphology of GES-1, SGC-7901, and MGC-803 cells in monolayer and spheroid status. Scale bar, 50 μm. **D,** Flow cytometry analysis confirms the CD44+/CD54+ CSC subset in GCSCs (GCSC1 and GCSC2). **E,** Western

blot analysis of WNT2 protein expression in GCSCs grown as spheroids versus monolayer.

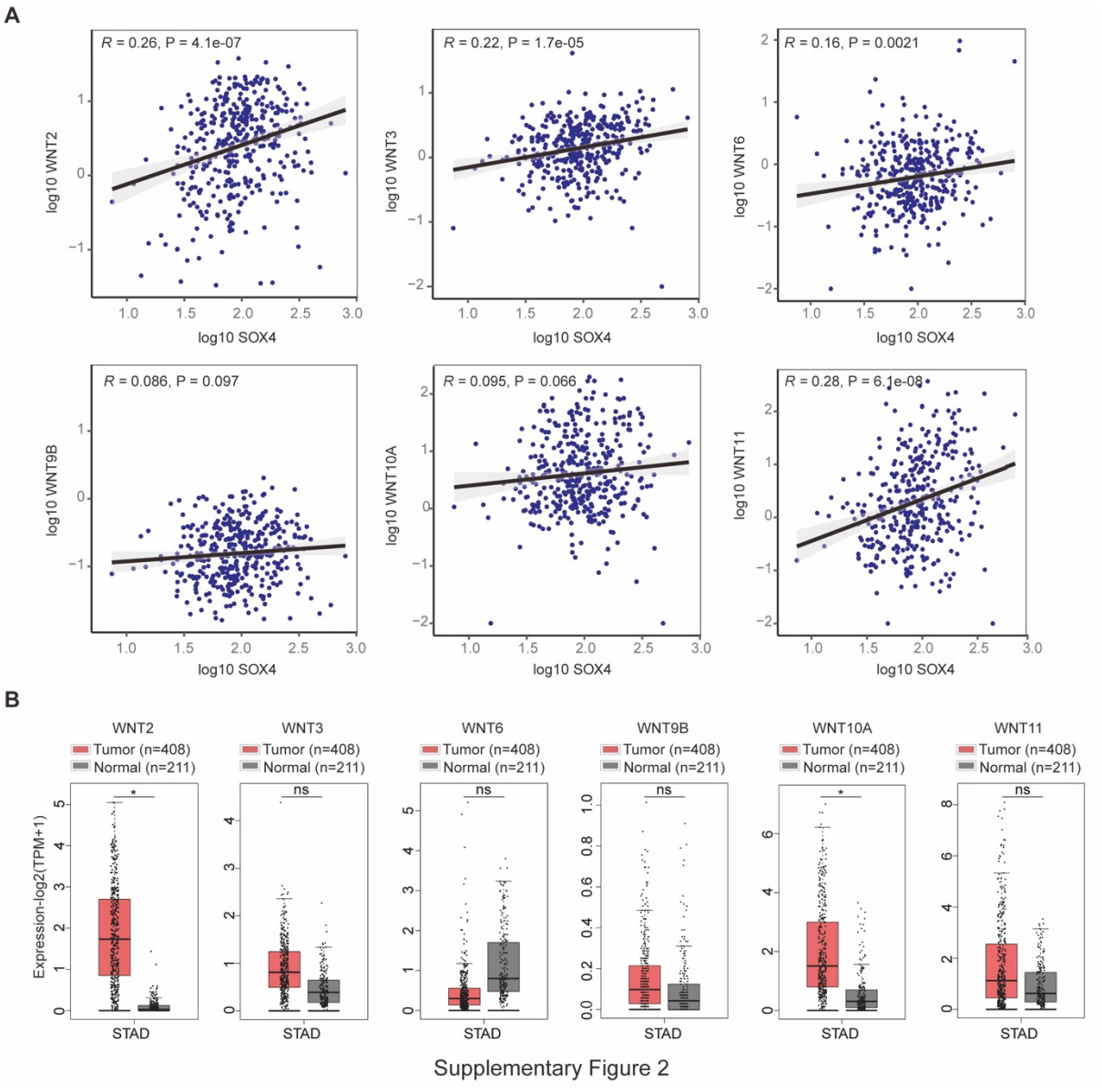

Supplementary Figure 2

Supplementary Fig. 2 SOX4 is positively correlated with WNT2 in GC (Related to Fig. 3)

A, Pearson's correlation analysis between the mRNA expression of *SOX4* and 6 potential SOX4-transactivated *WNT* genes (*WNT2*, *WNT3*, *WNT6*, *WNT9B*, *WNT10A*, and *WNT11*) based on the TCGA STAD dataset. **B,** The mRNA expression levels of *WNT2*, *WNT3*, *WNT6*, *WNT9B*, *WNT10A*, and *WNT11* between GC tumor tissues (Tumor) and normal gastric tissues (Normal) based on the GEPIA STAD dataset. The

error bars are presented as the means ± SD. ns, not significant; *, $P < 0.05$. STAD, stomach adenocarcinoma. TPM, transcripts per million.

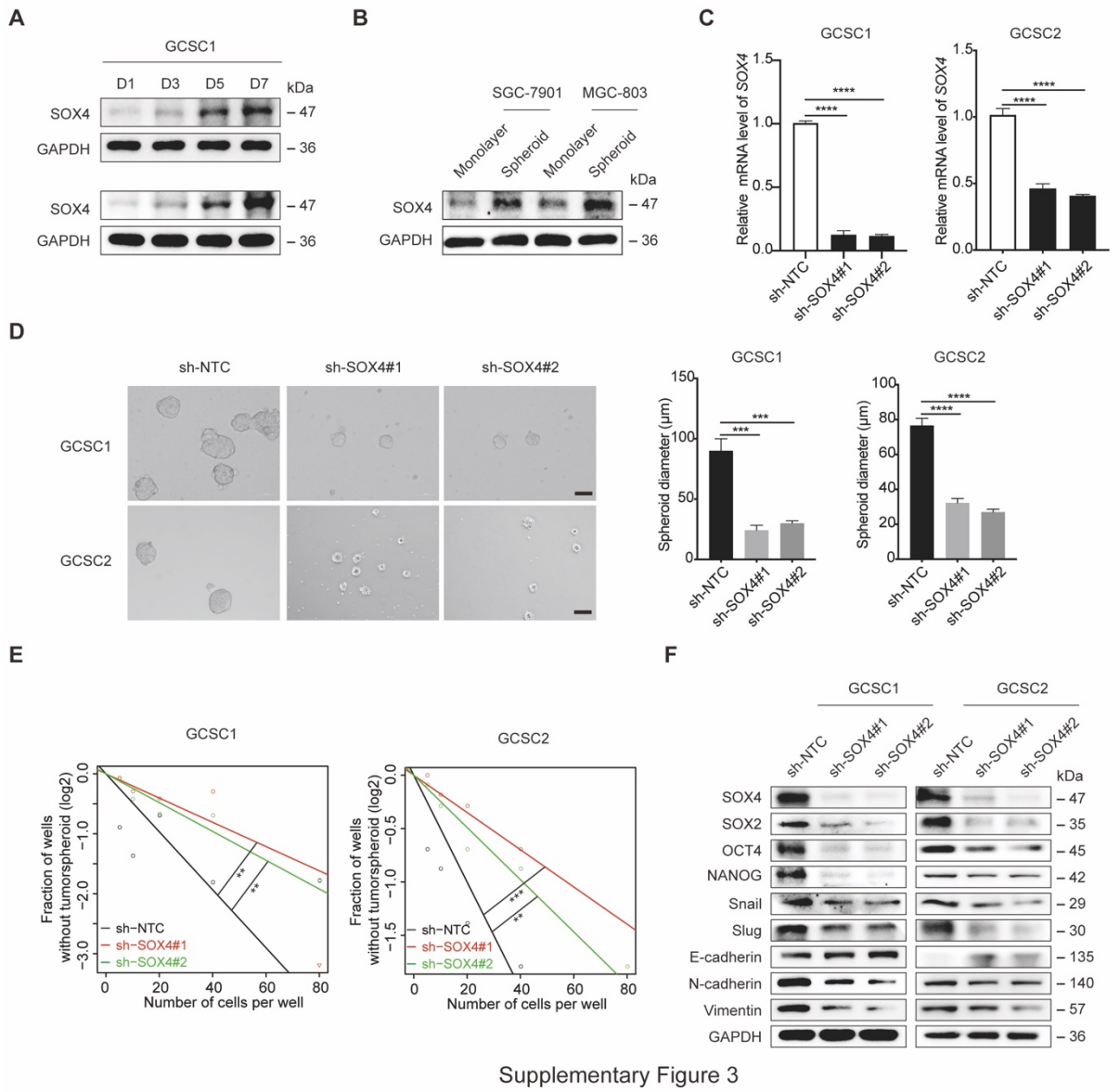

Supplementary Figure 3

Supplementary Fig. 3 SOX4 promotes GCSC stemness and EMT (Related to Fig. 4)

A, Western blot showing protein levels of SOX4 in GCSCs on day (D) 1, 3, 5 and 7. **B,** Western blot showing SOX4 protein expression in SGC-7901 and MGC-803 grown in monolayer versus spheroids. **C,** Results of qPCR of SOX4 mRNA from SOX4-silenced GCSCs. **D,** Representative photomicrographs of SOX4-knockdown GCSCs indicates that silencing of SOX4 decreased spheroid formation of GCSCs. scale bar, 50 μm. **E,** *In vitro* limiting dilution assays showing effects of SOX4-knockdown on the

spheroid formation of GCSCs. **F,** Western blot analysis of SOX4, stemness- and EMT-associated markers in SOX4-silenced GCSCs. The error bars are presented as the means ± SD. **, $P < 0.01$; ***, $P < 0.001$; ****, $P < 0.0001$.

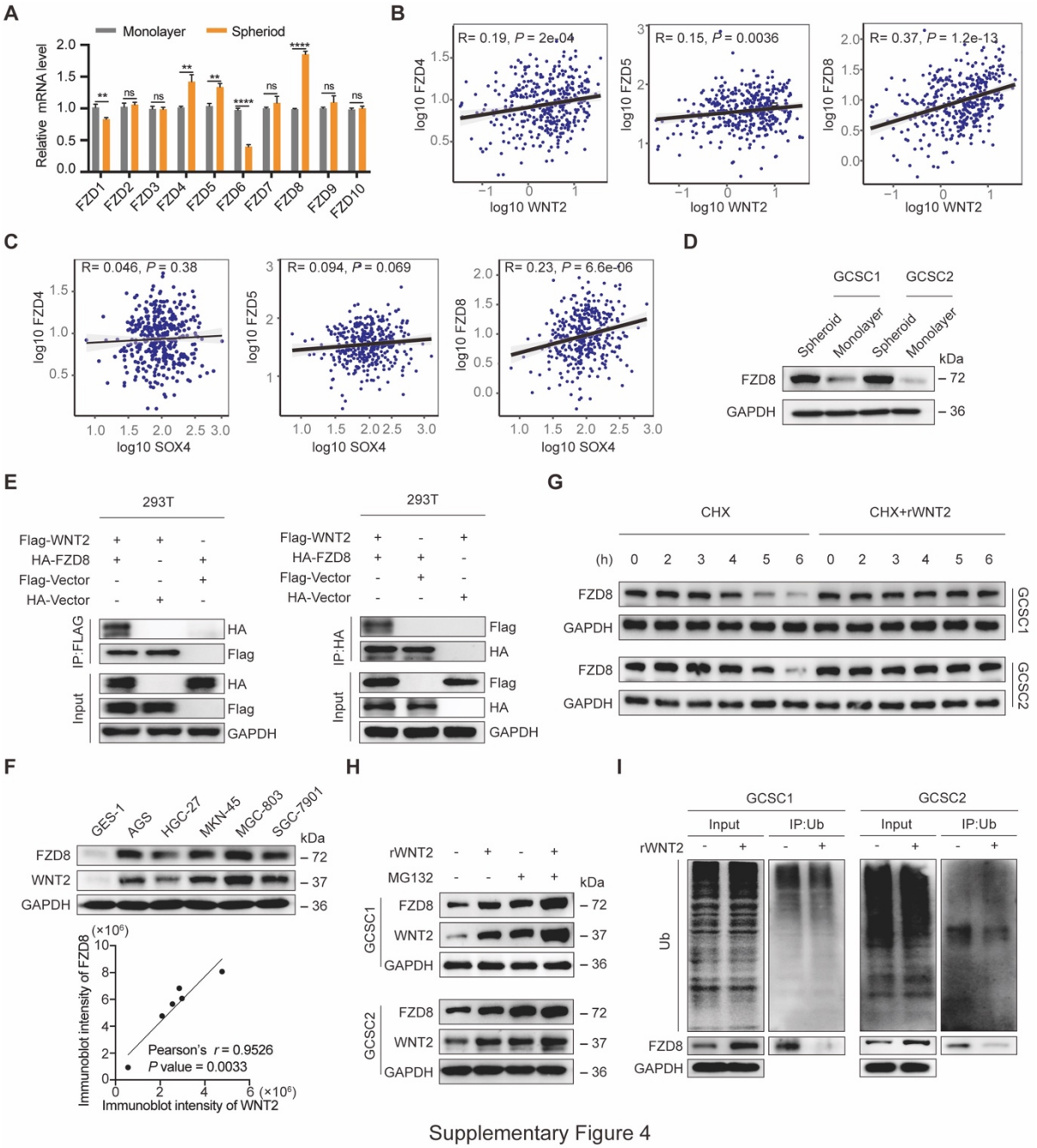

Supplementary Figure 4

Supplementary Fig. 4 WNT2 binds to and stabilizes FZD8 receptor by inhibiting its ubiquitination in GCSCs (Related to Fig. 5)

A, qPCR analysis showing the expression FZDs in spheroid and monolayer of GCSCs. **B,** Pearson's correlation analysis between the mRNA expression levels of *WNT2* and

3 potential WNT2-regulating *FZD*s (*FZD4*, *FZD5* and *FZD8*) in the TCGA STAD database. **C,** Pearson's correlation analysis between the mRNA expression levels of *SOX4* and 3 potential WNT2-regulating *FZD*s (*FZD4*, *FZD5* and *FZD8*) in the TCGA STAD database. **D,** Western blot demonstrated the protein expression level of FZD8 in GCSCs grown as spheroids versus monolayer. **E,** Co-immunoprecipitation of Flag-tagged WNT2 and HA-tagged FZD8 in 293T cells. Whole cell lysate (input) proteins were detected using western blot analysis. **F,** Western blot of WNT2 and FZD8 protein expression in GES-1 and 5 GC cell lines. Pearson's correlation between WNT2 and FZD8 protein expression in GES-1 and gastric cancer cell lines. **G,** FZD8 protein levels at the hour (h) 0, 2, 3, 4, 5 and 6 in GCSCs treated with cycloheximide (CHX, 100 μM) and recombinant WNT2 protein (50 ng/ml). **H,** Western blot analysis of FZD8 and WNT2 protein levels in GCSCs subjected to control or recombinant WNT2 protein treatment (50 ng/ml) after treatment or not with MG132 (100 μM) for 9 h. **I,** Immunoblots showing WNT2 inhibition of FZD8 ubiquitination. Total cell lysates extracted from GCSCs were immunoprecipitated with a ubiquitin (Ub) antibody and incubated with antibodies against the indicated proteins. Non-specific mouse IgG was used as a control. The error bars are presented as the means ± SD. ns, not significant; **, $P < 0.01$; ****, $P < 0.0001$.

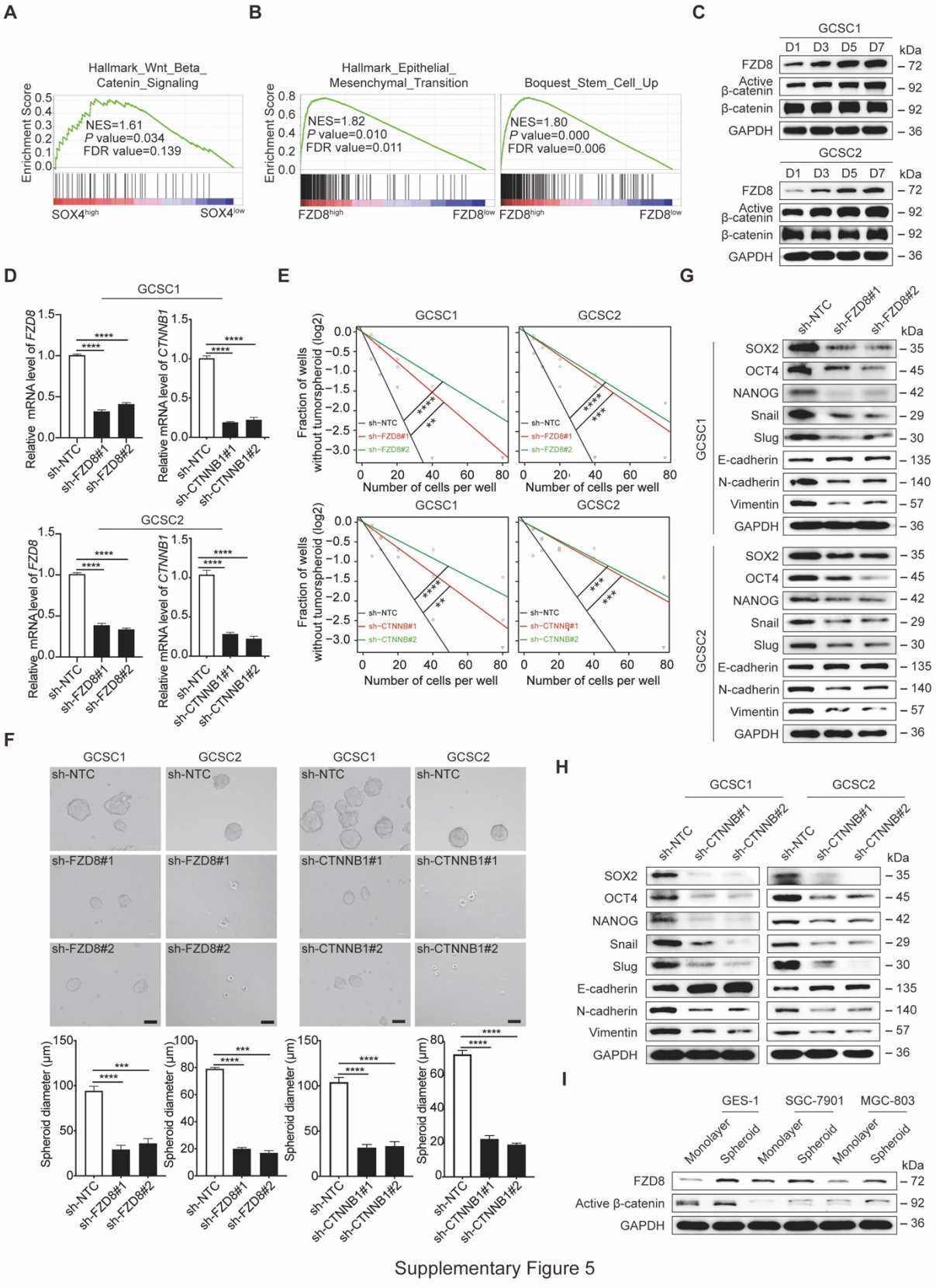

Supplementary Figure 5

Supplementary Fig. 5 FZD8 and CTNNB1 maintain stemness concomitantly in GCSCs (Related to Fig. 5)

A, GSEA analysis of WNT/β-catenin signaling pathway gene modulation by SOX4 in gastric cancer samples from the TCGA dataset (n = 415). **B,** GSEA enrichment plots of expression of genes associated with EMT and stem cells in high FZD8 versus low FZD8 expressing gastric cancer samples in the TCGA dataset (n = 415). **C,** Expression levels of FZD8, active β-catenin, and β-catenin proteins as examined by western blot in GCSCs on day (D) 1, 3, 5, and 7. **D,** Transcriptional levels of FZD8 and CTNNB1 in GCSCs transfected with FDZ8 and CTNNB1 shRNAs (sh-CTNNB1#1 or sh-CTNNB1#2) or control shRNA (sh-NTC) as measured by qPCR. **E,** *In vitro* limiting dilution assay results showing effects of FZD8 or β-catenin in GCSCs. **F,** Tumor spheroid formation assays indicating that silencing FZD8 or CTNNB1 decreased sphere formation of GCSCs. Representative photomicrographs of GCSCs transfected with sh-RNA; scale bar, 50 μm. **G,** Immunoblots of stemness- and EMT-related proteins in FZD8-silenced GCSCs. **H,** Western blot of stemness- and EMT-related proteins in lysates prepared from CTNNB1-silenced GCSCs. **I,** Western blot of FZD8 and active β-catenin protein expression in GES-1, SGC-7901, and MGC-803 cells grown as spheroids versus monolayer. The error bars are presented as the means ± SD. **, $P < 0.01$; ***, $P < 0.001$; ****, $P < 0.0001$.

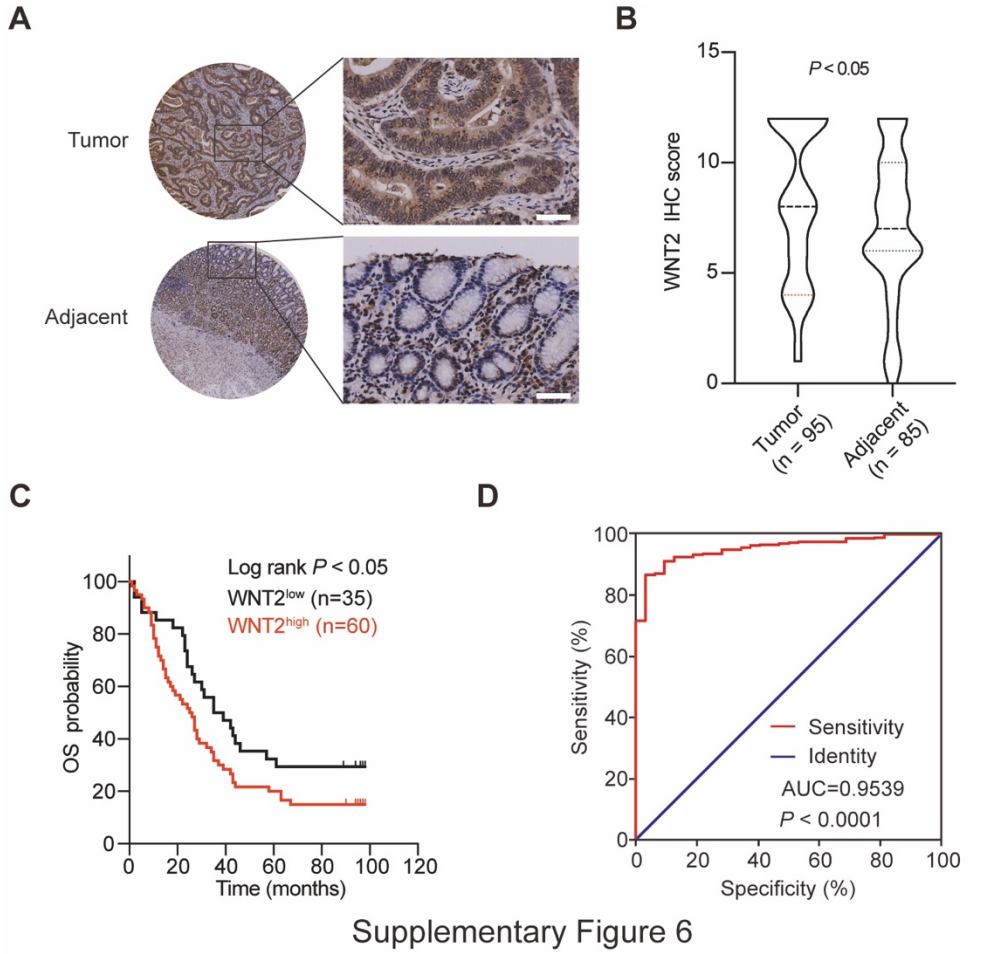

Supplementary Figure 6

Supplementary Fig. 6 Elevation of WNT2 is associated with poor prognosis in GC patients (Related to Fig. 5)

A, Representative IHC images of WNT2 protein in tumor tissues and adjacent normal gastric tissues from the GC TMA cohort. Scale bar, 50 μm. **B,** Statistic analysis of WNT2 IHC staining score in tumor tissues (n = 95) versus adjacent tumor tissues (n = 85) of GC. **C,** Kaplan–Meier analysis stratified according to the WNT2 protein expression in 95 informative GC tumor samples (P = 0.0489 using the log-rank test). **D,** ROC analysis demonstrated that WNT2 mRNA expression levels were specific and sensitive biomarkers for GC detection based on the TCGA STAD dataset (AUC = 0.9539, $P < 0.0001$).

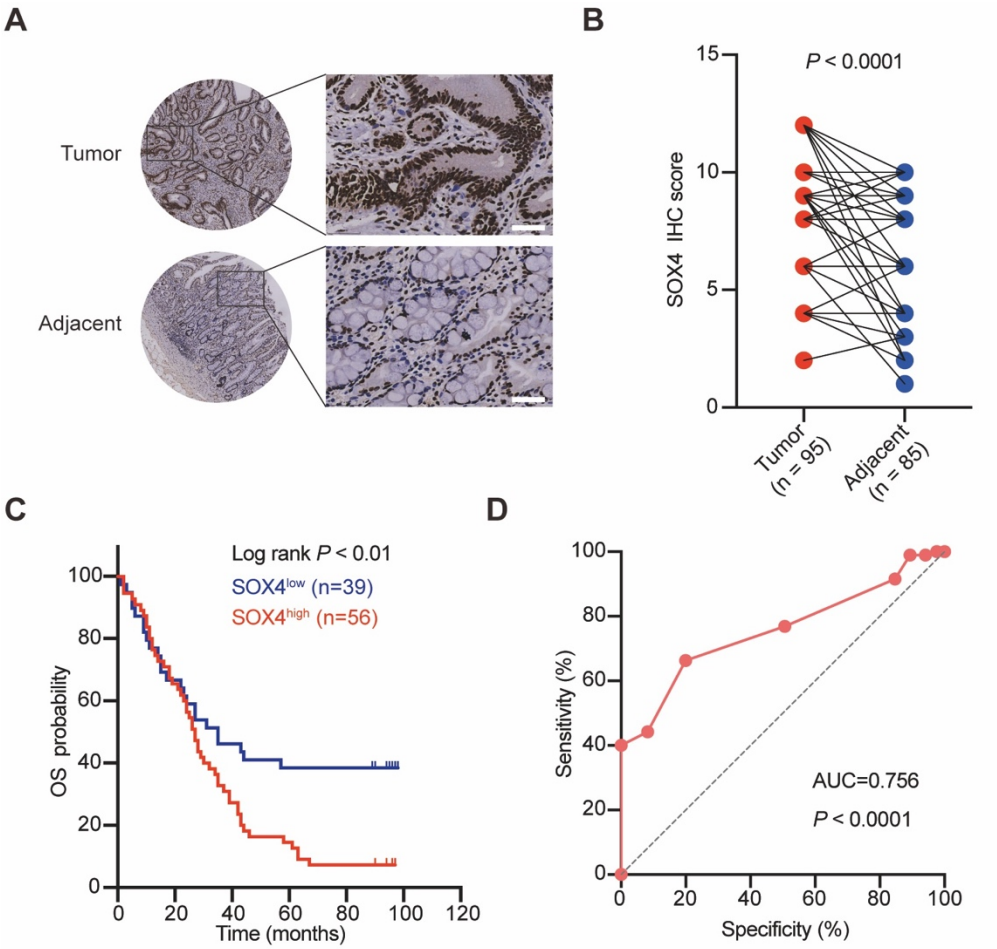

Supplementary Figure 7

Supplementary Fig. 7 Overexpression of SOX4 is associated with poor prognosis in gastric cancer cohorts (Related to Fig. 5)

A, Representative IHC images of SOX4 protein in tumor tissues and adjacent normal gastric tissues from the GC TMA cohort. Scale bar, 50 μm. **B,** Statistic analysis of SOX4 IHC staining score in tumor tissues (n = 95) versus adjacent tumor tissues (n = 85) of GC. **C,** Kaplan–Meier analysis stratified according to the SOX4 protein expression in 95 informative GC tumor samples (P = 0.0084 using the log-rank test). **D,** ROC analysis demonstrated that SOX4 mRNA expression levels were specific and sensitive biomarkers for GC detection based on the TCGA STAD dataset (AUC = 0.756, $P < 0.0001$).

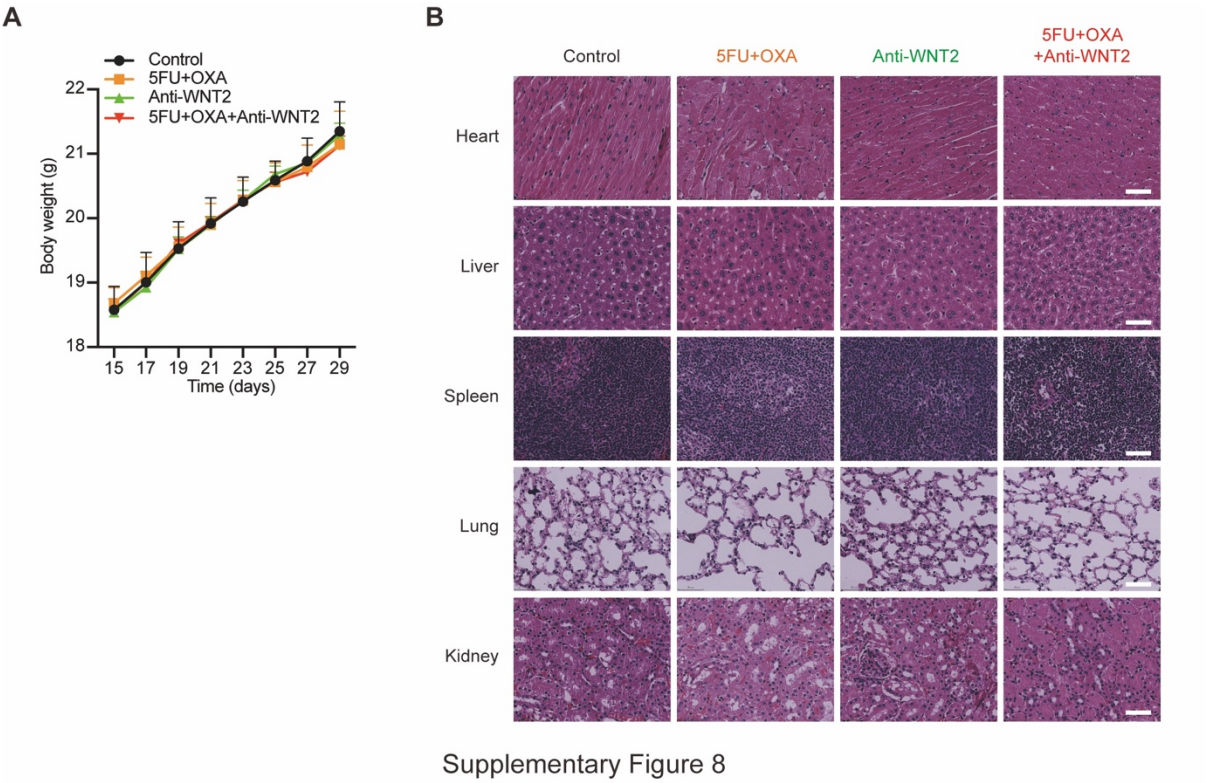

Supplementary Figure 8

Supplementary Fig. 8 Anti-WNT2 mAb enhances chemotherapeutic efficacy in mice bearing GCSC xenografts (Related to Fig. 6)

A, Body weight of mice in the indicated treatment groups bearing GCSC xenografts as monitored every 2 days. **B,** H&E staining of mouse vital organs confirmed a normal pathological phenotype; scale bar, 50 μm. The error bars are presented as the means ± SD.

Supplemental Tables

Table S1: Clinicopathological correlation of WNT2 expression in gastric cancer (n=95)

Variables	Total	WNT2 expression[a]		*P* value[b]
		High	Low	
Age (y)				0.3457
≤ 65	44	30 (68.2%)	14 (31.8%)	
> 65	51	30 (58.8%)	21 (41.2%)	
Gender				0.7938
Female	23	14 (60.9%)	9 (39.1%)	
Male	72	46 (63.9%)	26 (36.1%)	
Differentiation				0.0207*
Well/Moderate	25	11 (44.0%)	14 (56.0%)	
Poor	70	49 (70.0%)	21 (30.0%)	
TNM stage[c]				0.0244*
I and II	35	17 (48.6%)	18 (51.4%)	
III and IV	60	43 (71.7%)	17 (28.3%)	
Tumor stage				0.0987
T1 and T2	12	5 (41.7%)	7 (58.3%)	
T3 and T4	83	55 (66.3%)	28 (33.7%)	
Lymph nodes metastasis(N)				0.3947
Absent	20	11 (55.0%)	9 (45.0%)	
Present	75	49 (65.3%)	26 (34.7%)	
Distant metastasis(M)				0.5773
M0	91	58 (63.7%)	33 (36.2%)	
M1	4	2 (50.0%)	2 (50.0%)	

a: WNT2 IHC score ≥ 8 as high expression; < 8 as low expression

b: Pearson χ^2 test

c: AJCC/UICC TNM staging system

*$P < 0.05$

Table S2: Clinicopathological correlation of SOX4 expression in gastric cancer (n=95)

Variables	Total	SOX4 expression[a]		*P* value[b]
		High	Low	
Age (y)				0.0996
≤ 65	44	22 (50.0%)	22 (50.0%)	
> 65	51	34 (66.7%)	17 (33.3%)	
Gender				0.2130
Female	23	11 (47.8%)	12 (52.2%)	
Male	72	45 (62.5%)	27 (37.5%)	
Differentiation				0.7464
Well/Moderate	36	23 (63.9%)	13 (36.1%)	
Poor	59	33 (55.9%)	26 (44.1%)	
TNM stage[c]				0.7859
I and II	23	13 (56.5%)	10 (43.5%)	
III and IV	72	43 (59.7%)	29 (40.3%)	
Tumor stage				0.0536
T1 and T2	12	4 (33.3%)	8 (66.7%)	
T3 and T4	83	52 (62.7%)	31(37.3%)	
Lymph nodes metastasis(N)				0.3600
Absent	75	46 (61.3%)	29 (38.7%)	
Present	20	10 (50.0%)	10 (50.0%)	
Distant metastasis(M)				0.1585
M0	91	55 (60.4%)	36 (39.6%)	
M1	4	1 (50.0%)	3 (50.0%)	

a: SOX4 IHC score ≥ 9 as high expression; < 9 as low expression

b: Pearson χ^2 test

c: AJCC/UICC TNM staging system

*$P < 0.05$

References

1 Hu Y, Smyth GK. ELDA: extreme limiting dilution analysis for comparing depleted and enriched populations in stem cell and other assays. *J Immunol Methods* 2009; **347**: 70–78.